

Intrinsic low-temperature magnetic properties on the ultra-clean UTe₂ with $T_c = 2.1$ K revealed by ¹²⁵Te NMR

Hiroki Matsumura,^{1,*} Shunsaku Kitagawa,^{1,†} Shiki Ogata,¹ Riku Matsubayashi,¹ Hiroki Fujibayashi,¹
Katsuki Kinjo,^{1,2} Kenji Ishida,¹ Yo Tokunaga,³ Hironori Sakai,³ Shinsaku Kambe,³ Ai Nakamura,⁴
Yusei Shimizu,⁴ Yoshiya Homma,⁴ Dexin Li,⁴ Fuminori Honda,^{4,5} Atsushi Miyake,⁴ and Dai Aoki^{4,6}

¹*Department of Physics, Graduate School of Science, Kyoto University, Kyoto 606-8502, Japan*

²*Institute of Multidisciplinary Research for Advanced Materials,
Tohoku University, Sendai, Miyagi 980-8577, Japan*

³*Advanced Science Research Center, Japan Atomic Energy Agency, Tokai, Ibaraki 319-1195, Japan*

⁴*Institute for Materials Research, Tohoku University, Oarai, Ibaraki 311-1313, Japan*

⁵*Central Institute of Radioisotope Science and Safety, Kyushu University, Fukuoka 819-0395, Japan*

⁶*Université Grenoble Alpes, CEA, IRIG, PHELIQS, F-38000 Grenoble, France*

(Dated: March 13, 2025)

To investigate the intrinsic magnetic properties of UTe₂, we performed ¹²⁵Te-NMR measurements on the ultra-clean single-crystalline UTe₂ with superconducting transition temperature $T_c = 2.1$ K and compared the results with those of the $T_c = 1.6$ K sample. The broadening of the linewidth of the NMR spectrum in the a -axis magnetic field and the low-temperature magnetic fluctuations observed in the 1.6 K sample are suppressed in the ultra-clean sample, indicating that such magnetic properties originate from a tiny amount of U deficiency. The present results suggest that the magnetic properties in UTe₂ are sensitive to the U deficiency. We also observed a peculiar angular dependence of the NMR quantities due to large magnetic anisotropy with the a -axis as the magnetic easy axis.

I. INTRODUCTION

In conventional superconductors, the electron-phonon interactions are the origin of an attractive force for the Cooper pairs[1]. On the other hand, in unconventional superconductors, the attractive force is not mediated by phonon, but by other interactions, such as magnetic interactions[2–14]. This also seems to be the case in the recently discovered superconductor UTe₂. UTe₂ is a uranium-based compound with a superconducting (SC) transition temperature of $T_c = 1.6 - 2.1$ K[15–17]. Although it does not exhibit a ferromagnetic transition, it shows many similarities to ferromagnetic superconductors[18–21], such as Ising magnetic anisotropy and a peculiar SC phase diagram[15, 22–33]. Thus, when it was first discovered, the realization of a spin-triplet SC state mediated by ferromagnetic fluctuations was pointed out[15]. In fact, strong ferromagnetic fluctuations were suggested from various measurements[15, 34–36]. On the other hand, inelastic neutron scattering experiments suggested the existence of antiferromagnetic fluctuations with $Q = (0, 0.57, 0)$ at ambient pressure[37, 38]. In addition, static antiferromagnetic order with $Q = (0.07, 0.67, 0)$ was found under pressure[39], implying that the magnetic properties of the normal state in UTe₂ are not simple. In addition, NMR measurements in the early-stage samples with $T_c \sim 1.6$ K (1.6 K sample) suggested that antiferromagnetic-type fluctuations develop at low temperatures due to a tiny amount of U deficiency[40, 41]. μ SR measurements also detected the spin freezing in UTe₂ samples with the residual electronic term in the specific heat[35, 42]. Therefore, high-quality samples are necessary to investigate the in-

trinsic magnetic properties of UTe₂.

Recently, an ultra-clean single-crystal sample (2.1 K sample) with a large increase in T_c to 2.1 K and almost zero residual electronic coefficient at 0 K is available due to an improvement in the synthesis method[45], as shown in Fig. 1(b). A low-temperature upturn in magnetic susceptibility for $H \parallel a$ observed in the 1.6 K sample[15, 46] is absent in the 2.1 K sample[47]. In addition to the magnetic properties, the relationship between T_c and the residual electronic term in the specific heat indicates that the 2.1 K sample is a disorder-free sample with intrinsic T_c in UTe₂[17, 47].

In this paper, we perform NMR measurements on this ultra-clean single-crystal sample and compare the results with those of the 1.6 K sample to investigate the intrinsic magnetic properties of UTe₂. Our NMR measurements reveal that the low-temperature magnetic anomalies observed in the 1.6 K sample are not observed in the 2.1 K samples.

II. EXPERIMENTAL

¹²⁵Te-enriched ultra-clean samples were prepared with the newly developed molten salt flux method[45]. Natural U and 99.9% ¹²⁵Te-enriched metals were used as starting materials for the present sample. The ferromagnetic U₇Te₁₂[48] is absent in our samples. The single crystals exhibit an SC transition at $T_c = 2.1$ K, which was determined with the specific heat and ac susceptibility measurements as shown in Fig. 1(b)[44, 49]. This is the highest T_c reported in UTe₂[17, 47]. This sample shows a quite small residual electronic term well below T_c , indicating that the increase in T_c is ascribed to the

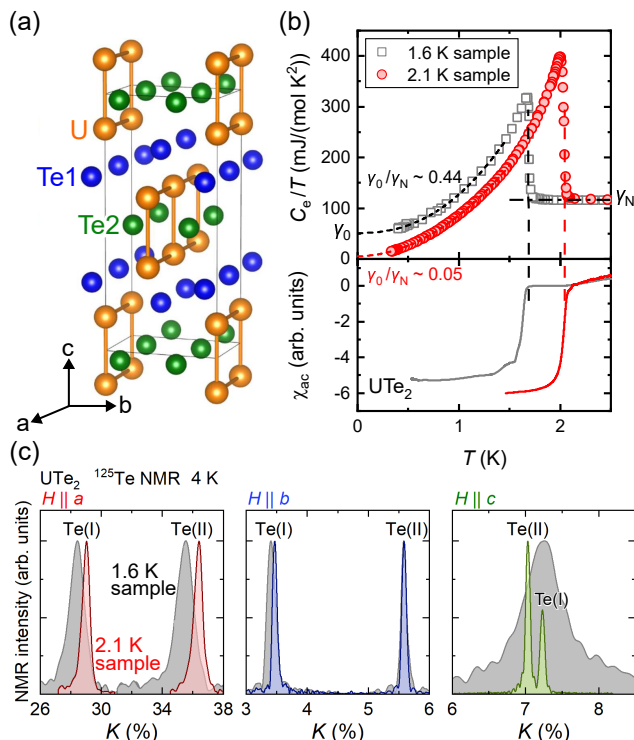


FIG. 1. (a) Crystal structure of UTe_2 drawn by VESTA[43]. (b) Temperature dependence of the electronic term of the specific heat divided by temperature C_e/T and the ac susceptibility measured with variation in resonance frequency of NMR tank circuits in the 1.6 and 2.1 K samples. The vertical and horizontal broken lines indicate T_c and the normal-state Sommerfeld coefficient γ_N , respectively. Residual-specific heat values for each sample, scaled by the normal state value, γ_0/γ_N were estimated by extrapolation of the full-gap behavior[44]. (c) ^{125}Te -NMR spectrum as a function of K measured in the 1.6 and 2.1 K samples when H is applied to three crystalline axes (a , b , and c). In $H \parallel c$, the 1.6 K sample shows the broad spectrum due to overlapping Te(I) and Te(II)-NMR peaks, but the two peaks were separated in the 2.1 K sample. All spectra were measured at 4 K.

reduction of the disorder due to the U deficiency[45, 50]. For comparison, we also performed NMR measurements in the early-stage 1.6 K sample grown by the chemical vapor transport method[16]. The 1.6 K sample is identical to that used in our previous study, and some of the data were already published[51, 52]. The ^{125}Te (nuclear spin $I = 1/2$, gyromagnetic ratio $^{125}\gamma/2\pi = 13.454$ MHz/T)-NMR measurements on the 2.1 K sample were performed on two same-batch single crystals of size $2 \times 1.2 \times 1$ mm³ for the ab and ac plane rotations and $3 \times 1 \times 0.5$ mm³ for the bc plane rotation. We reported that two ^{125}Te -NMR signals were observed in UTe_2 due to the presence of the two inequivalent crystallographic Te sites, as seen in Fig. 1(a). Note that the peak assignment [Te(I) and Te(II)] does not correspond to the crystallographic site (Te1 and Te2)[41]. The NMR spectra as a function of frequency were obtained using the Fourier transform of a

spin-echo signal observed after a radio-frequency pulse sequence at a fixed magnetic field. The NMR spectra are presented with the horizontal axis representing $K = (f - f_0)/f_0$. Here, $f_0 = (^{125}\gamma/2\pi)\mu_0 H$ is the reference frequency. The magnetic field was calibrated using a ^{65}Cu ($^{65}\gamma/2\pi = 12.089$ MHz/T)-NMR signal with the Knight shift $K_{\text{Cu}} = 0.2385\%$ from the NMR coil[53]. The sample was rotated in the ab , bc , and ac planes to precisely apply the magnetic field along each axis using a split-pair magnet with a single-axis rotator. The Knight shift and full width at half maximum (FWHM) were determined by the peak position and width at the half-maximum value of the NMR spectrum, respectively. In $H \parallel c$, the NMR signals of the two sites are quite close. Therefore, the FWHM was determined by fitting with a double Gaussian. A nuclear spin-lattice relaxation rate $1/T_1$ was evaluated by fitting the relaxation curve of the nuclear magnetization after the saturation to a theoretical function for the nuclear spin $I = 1/2$, which is a single exponential function.

III. RESULTS AND DISCUSSION

A. Knight shift and anomalous broadening of NMR linewidth

As shown in Fig. 1 (c), the NMR spectra for the 2.1 K sample are sharper in all crystallographic axes (a , b , and c) than those for the 1.6 K sample[51, 54], indicating the improvement of the sample quality. In particular, note that the sharpening of the NMR spectrum along the c axis separates between the Te(I) and Te(II) peaks. In contrast to linewidth, as shown in Figs. 2(a)-(c), the Knight shifts for both the 1.6 K and 2.1 K samples exhibit almost the same behavior, implying no significant change in static magnetic properties. Slight differences in peak positions between the samples [Fig. 1 (c)] may originate from misalignment of field direction.

The most significant contrast between the 1.6 K and 2.1 K samples lies in the linewidth of the NMR spectrum along the a axis. Previous investigations revealed a substantial increase in linewidth, relative to the Knight-shift value, below 30 K for the 1.6 K sample[40, 41]. The linewidth of the NMR spectrum is a physical quantity that reflects the distribution of magnetic susceptibility, and in the paramagnetic state, the magnetic susceptibility is proportional to the Knight shift. Consequently, the substantial increase in linewidth compared to the Knight shift suggests the presence of the distribution of staggered magnetic susceptibility. As shown in Fig. 2(a), in the 2.1 K sample, an increase in FWHM at lower temperatures is also observed compared to the Knight shift, although this difference is smaller than that observed in the 1.6 K sample[40]. Previous studies have proposed that this increase in FWHM is caused by the breaking of the magnetic correlations due to the tiny amount of U deficiency. In the 2.1 K sample, the reduction in the

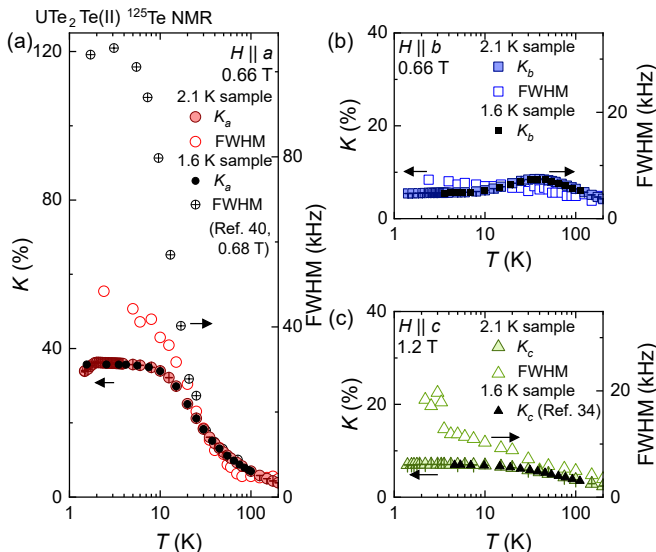


FIG. 2. Temperature dependence of Knight shift K and full width at half maximum (FWHM) at the Te(II) site for (a) $H \parallel a$, (b) $H \parallel b$, and (c) $H \parallel c$. We also plot the data in the 1.6 K sample for comparison.

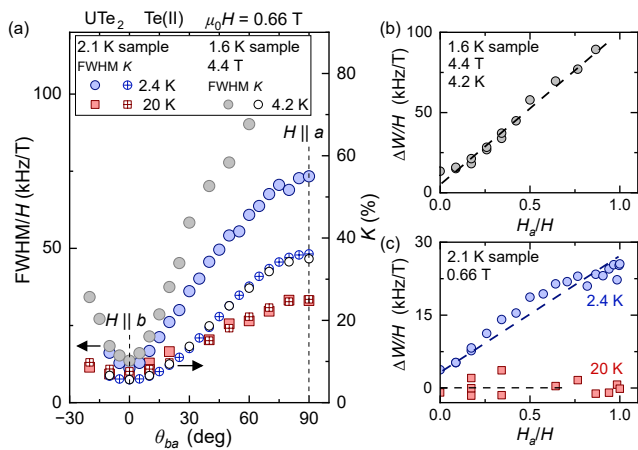


FIG. 3. (a) Variation in linewidth of the NMR spectrum and Knight shift at the Te(II) site against the magnetic field angle in the ab -plane measured at 2.4 K and 20 K. The applied magnetic field is 0.66 T. The broken lines indicate $\theta_{ba} = 0^\circ$ ($H \parallel b$) and 90° ($H \parallel a$). We also plotted the result at 4 K and 4.4 T in the 1.6 K samples with gray color for comparison. The a -axis projected field dependence of the anomalous broadening in FWHM ΔW divided by H in the 1.6 K sample (b) and the 2.1 K sample (c). The broken lines are guides for the eye.

U deficiency due to improved sample quality seems to suppress the increase in FWHM, providing a consistent explanation. It is noted that, for $H \parallel b$ and c , such an effect was smaller, although FWHM is not proportional to K at low temperatures, as shown in Figs. 2(b) and 2(c). In particular, the FWHM is larger than the Knight shift at low temperatures for $H \parallel c$. This is due to the overlap between the Te(I)- and Te(II)-NMR spectra, which makes the evaluation more difficult.

The anomalous increase in linewidth was observed in magnetic field angle dependence as well. Figure 3(a) illustrates the variation in FWHM of the NMR spectrum and Knight shift at the Te(II) site against the magnetic field angle in the ab -plane measured at 2.4 K and 20 K. We also plotted the result at 4 K in the 1.6 K sample for comparison. At 20 K, the observed angular dependence of linewidth around the b axis is smooth and scaled with the Knight shift, which is expected in the normal state. In contrast, at 2.4 K, a kink in linewidth was observed at $H \parallel b$. This is likely due to the additional linewidth broadening being proportional to the magnetic field along the a axis, as reported in the previous studies[40]. To highlight this additional broadening in FWHM, we plotted $\Delta W = \text{FWHM} - \alpha K$ divided by H as a function of the a -axis projected magnetic field $H_a = H \sin \theta_{ba}$, where $\alpha = 0.92$ is the same value between the 1.6 K sample and 2.1 K sample, and θ_{ba} represents the angle between the magnetic field direction and the b axis. As shown in Figs. 3 (b) and 3(c), $\Delta W/H$ is almost linearly proportional to H_a , indicating that the increase is induced by H_a . In the 2.1 K sample, the slope $\Delta W/H_a = 25 \text{ kHz/T}$ is considerably smaller than that in the 1.6 K sample ($\Delta W/H_a = 100 \text{ kHz/T}$), implying the high quality of the 2.1 K sample. To clarify the origin of the additional broadening in FWHM, a more detailed investigation into the sample dependence and magnetic field dependence is crucial. These aspects will be addressed in future work.

B. Unusual angular dependence of Knight shift due to large magnetic anisotropy

From the angular dependence of the Knight shift at low temperatures, we found that the angular rotation from the b axis or c axis to the a axis reflects the large magnetic anisotropy in UTe_2 . In general, the Knight shift K is defined as

$$K \equiv \frac{|\mathbf{H}_{\text{ext}} + \mathbf{H}_{\text{hf}}| - |\mathbf{H}_{\text{ext}}|}{|\mathbf{H}_{\text{ext}}|}. \quad (1)$$

Here, $\mathbf{H}_{\text{ext(hf)}}$ is the applied(hyperfine) magnetic field. When we assume that the \mathbf{H}_{hf} is parallel to \mathbf{H}_{ext} , the magnetic field angle dependence of the Knight shift K_θ in the ij plane can be expressed as a projection from each crystal axis component as follows:

$$K_\theta^{\text{normal}} = K_i \cos^2 \theta_{ij} + K_j \sin^2 \theta_{ij}. \quad (2)$$

Here, $K_{i(j)}$ is the Knight shift along the $i(j)$ axis, and θ_{ij} is defined as the angle from the i axis to the j axis. As shown in Fig. 4(a), the angular dependence of the Knight shift in the ab plane of UTe_2 agrees well with eq.(2) at 40 K, but it deviates at 2.4 K. To elucidate this difference, we subtracted the normal angle-dependent component, K_θ^{normal} , from the experimental data and present the result in Fig. 4(b). The deviation part of the Knight shift increases smoothly with increasing θ_{ba} , peaks at

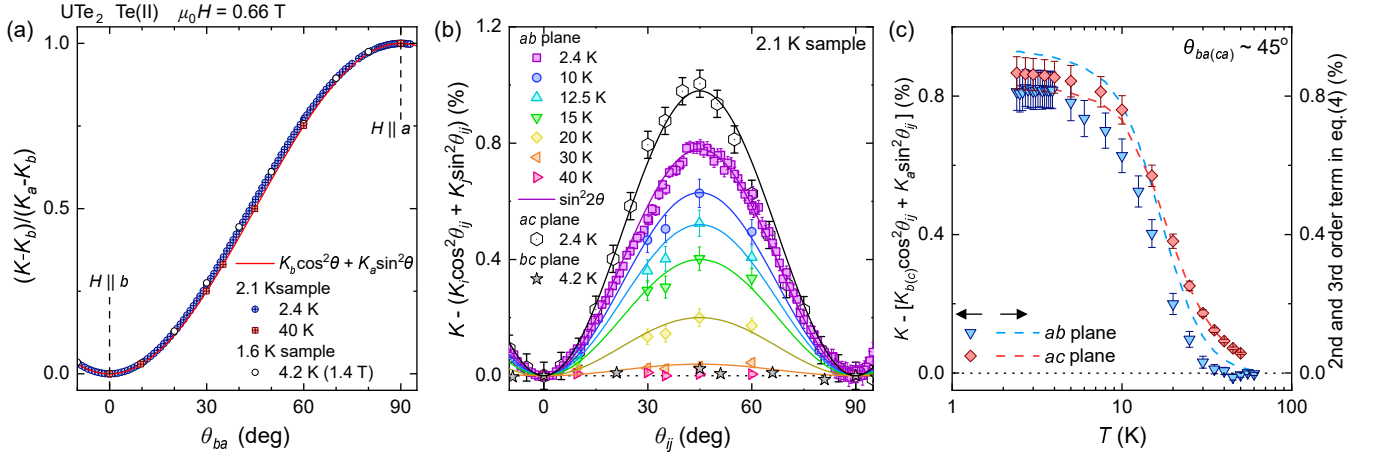


FIG. 4. (a) Magnetic field angle dependence of Knight shift normalized by K_a and K_b at 2.4 K and 40 K for the 2.1 K sample and 4.2 K for the 1.6 K sample. The applied magnetic field is 0.66 T and 1.4 T in the 2.1 K and the 1.6 K sample, respectively. The broken lines indicate $\theta = 0^\circ (H \parallel b)$ and $90^\circ (H \parallel a)$. The solid curve indicates theoretical equation for conventional materials ($K_\theta^{\text{normal}} = K_b \cos^2 \theta + K_a \sin^2 \theta$). (b) Magnetic field angle dependence of anomalous part of Knight shift at various temperatures in the 2.1 K sample. We also plot the data rotated in the ac and bc planes. The solid curves indicate the $\sin^2 2\theta_{ij}$ curve. (c) Temperature dependence of anomalous part of Knight shift at $\theta_{ba(ca)} = 45^\circ$ and the second- and third-order term in eq. (4). The dotted lines indicate $K = 0\%$.

$\theta_{ba} = 45^\circ$, and then decreases toward the a axis, following a $\sin^2 2\theta_{ba}$. As shown in Figs. 4(a) and 4(b), such an angular dependence is also observed in the ac plane, at the Te(I) site (not shown), and in the 1.6 K sample, but not in the bc plane. Although the higher-order angle-dependent term is sometimes discussed as the emergence of nonlinear magnetic susceptibility[55–58], we consider that this anomaly on UTe_2 originates from the directional difference between \mathbf{H}_{hf} and \mathbf{H}_{ext} caused by the large anisotropy of the Knight shift. Using eq.(1) and $H_{\text{hf},i} = K_i H_{\text{ext},i}$ [34, 41], K_θ in the ab plane can be written as,

$$K_\theta = \sqrt{(1 + K_b)^2 \cos^2 \theta_{ba} + (1 + K_a)^2 \sin^2 \theta_{ba}} - 1. \quad (3)$$

Expanding in a Maclaurin series assuming K_a and K_b are small, we get that

$$\begin{aligned} K_\theta &\sim K_b \cos^2 \theta_{ba} + K_a \sin^2 \theta_{ba} \\ &+ \frac{1}{8}(K_a - K_b)^2 \sin^2 2\theta_{ba} \\ &- \frac{1}{8} \sin^2 2\theta_{ba} [K_a^3 \cos^2 \theta_{ba} - K_a^2 K_b (3 \cos^2 \theta_{ba} - 1) \\ &- K_a K_b^2 (3 \sin^2 \theta_{ba} - 1) + K_b^3 \sin^2 \theta_{ba}] \end{aligned} \quad (4)$$

within the third-order expression. The second-order values of $\frac{1}{8}(K_a - K_b)^2 = 1.2\%$ and $\frac{1}{8}(K_a - K_c)^2 = 1.1\%$ are almost comparable with the amplitude of the $\sin^2 2\theta$ term $\sim 0.8\%$ and $\sim 0.9\%$, respectively. A slight difference may come from the misalignment of the angle and/or the higher-order term contributions. On the other hand, the value of $\frac{1}{8}(K_c - K_b)^2 = 0.01\%$ is negligible. Figure 4(c) shows the temperature dependence of the anomalous part of the Knight shift at $\theta \sim 45^\circ$ together with the second-

and third-order term in eq. (4). These components develop below 40 K and saturate below 4 K, which are similar to each other. The magnetic anisotropy of UTe_2 is exceptionally large, making conventional approximations inapplicable and suggesting that the higher-order angular dependence is observed.

C. Magnetic fluctuations

There are also differences in magnetic fluctuations observed in the 1.6 K and 2.1 K samples. Figures 5 (a)-(c) depict the temperature dependence of the nuclear spin-lattice relaxation rate $1/T_1 T$ for each crystallographic axis (a, b, c) along with the data in the 1.6 K sample[41] for comparison. In the 2.1 K sample, the sharper NMR linewidth allows us to measure the site dependence of $1/T_1$ for $H \parallel c$ at low temperatures. While the high-temperature behavior is consistent across the samples, there are clear distinctions in the low-temperature region. For the b axis, $1/T_1 T$ in the 1.6 K sample is almost constant below 10 K[41, 59, 60], whereas that in the 2.1 K sample, especially at the Te(I) site, exhibits a broad maximum at around 15 K with relatively smaller values. This temperature might be related to a broad Schottky-like anomaly observed in the various thermodynamic, transport probes[61–63] and the peak of the nuclear spin-spin relaxation rate $1/T_2$ [40]. Additionally, the increase observed below 5 K in the 1.6 K sample is absent in the 2.1 K sample.

In general, $1/T_1 T$ detects magnetic fluctuations per-

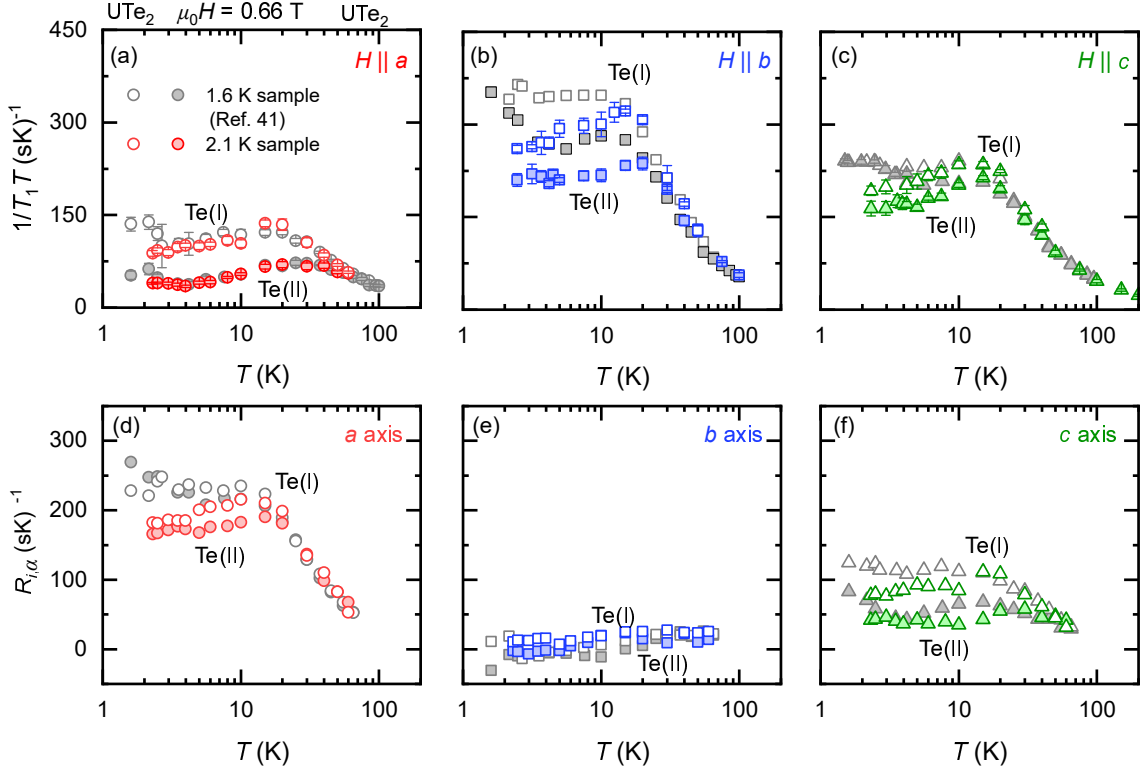


FIG. 5. Temperature dependence of $1/T_1T$ at Te(I) and Te(II) for (a) $H \parallel a$, (b) $H \parallel b$, and (c) $H \parallel c$ in the 2.1 K sample of UTe_2 . We also plotted the results in the 1.6 K samples with gray color for comparison. Temperature dependence of (d) $R_{i,a}$, (e) $R_{i,b}$, and (f) $R_{i,c}$ ($i = \text{I and II}$) evaluated from the data shown in the upper panel.

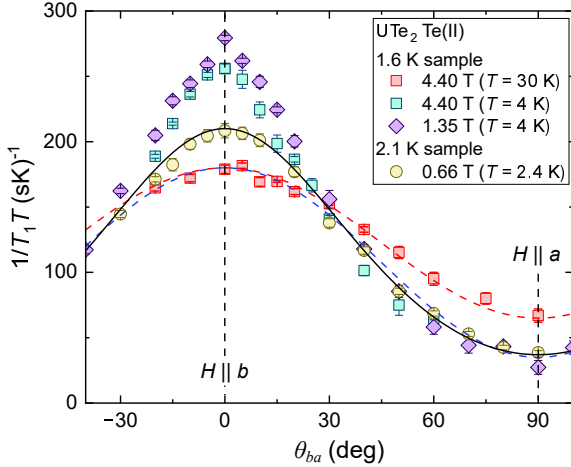


FIG. 6. Variation in $1/T_1T$ at the Te(II) site against the magnetic field angle in the ab -plane for various conditions. The broken lines indicate $\theta_{ba} = 0^\circ$ ($H \parallel b$) and 90° ($H \parallel a$). The broken (solid) curves are theoretical formulas expressed as Eq.(6) [(7)].

pendicular to the magnetic field expressed as,

$$R_{i,\alpha} = \sum_{\mathbf{q}, \xi} A_i^{\alpha\xi}(\mathbf{q})^2 \frac{\chi''_{\xi}(\mathbf{q}, \omega_N)}{\omega_N}, \quad (5)$$

where ω_N is the NMR frequency, $\chi''_{\xi}(\mathbf{q}, \omega_N)$ is the imaginary part of the dynamics susceptibility along $\xi = a, b, \text{ and } c$, and $A_i^{\alpha\xi}(\mathbf{q})$ is a \mathbf{q} -dependent hyperfine coupling tensor at the Te(i) ($i = \text{I, and II}$) site. Using this equation, magnetic fluctuations along each axis (a, b, c) can be extracted from each $1/T_1T$ data, as shown in Figs. 5 (d)-(f) with results for the 1.6 K sample. The b -axis spin fluctuations are small, resulting in no observable sample dependence. On the other hand, fluctuations along the a and c axes are suppressed in the 2.1 K sample compared to the 1.6 K sample. This suggests that the enhancement in the a - and c -axes magnetic fluctuations below 4 K is associated with the U deficiency and that the high quality of the 2.1 K sample led to the suppression of these fluctuations. The suppression of low-temperature fluctuations in high-quality samples was also observed in recent muon spin relaxation measurements[35, 64].

As the site dependence of $1/T_1$ under the c -axis magnetic field can be measured in the 2.1 K sample, we reveal that a -axis fluctuations also exhibit site dependence. The temperature dependence of $R_{i,\alpha}$ roughly corresponds to that of the Knight shift[41], suggesting the predominance of ferromagnetic ($q = 0$) correlations. On the other hand, for the a -axis, the static magnetic susceptibility at the Te(II) site is larger than that at the Te(I) site[41], while spin fluctuations at the Te(II) site are smaller than those at the Te(I) site. Furthermore,

despite almost the site-independent static magnetic susceptibility along the c axis, c -axis spin fluctuations are more pronounced at the Te(I) site. It is considered that the difference between the static susceptibility and the spin fluctuations originates from the difference in the q -dependent hyperfine coupling tensor $A_i^{\alpha\xi}(\mathbf{q})$. While the static susceptibility is related to the $q = 0$ component, the spin fluctuation detects all q components. Therefore, these experimental results suggest the coexistence of a ferromagnetic and an antiferromagnetic correlation with $q \neq 0$ in UTe_2 , which is consistent with the antiferromagnetic fluctuations with $Q = (0, 0.57, 0)$ observed in the neutron measurements[38].

The low-temperature magnetic fluctuations in the 1.6 K sample are also reflected in the magnetic field angle dependence of $1/T_1T$, as shown in Fig. 6. The angle dependence of $1/T_1T(\theta)$ typically exhibits similar angle dependence to the Knight shift in the normal state. In the 1.6 K sample, the experimental data at 30 K can be fitted well with a theoretical formula described as,

$$\frac{1}{T_1T}(\theta_{ba}) = \left(\frac{1}{T_1T}\right)_{H\parallel b} \cos^2 \theta_{ba} + \left(\frac{1}{T_1T}\right)_{H\parallel a} \sin^2 \theta_{ba}. \quad (6)$$

However, at 4 K, a kink behavior around the b axis was observed. This suggests the enhancement of magnetic excitations specifically around the b axis. Similarly to the additional increase in linewidth, the kink behavior in $1/T_1T$ is also attributed to the presence of the U deficiency. However, as shown in Fig. 6, the anomaly in $1/T_1T$ shows the same angle dependence, regardless of the magnetic field magnitude, indicating that it is related not to the magnitude of H_a but to the angles, unlike the case of the additional increase in linewidth. This result indicates that the enhancement of magnetic excitation around the b -axis is neither induced nor suppressed by H_a , in contrast to the behavior of UCoGe , where ferromagnetic fluctuations along the magnetic easy axis are suddenly suppressed with increasing the c -axis magnetic field[10, 65].

In the case of the 2.1 K sample, such kink behavior in $1/T_1T$ was not observed even at 2.4 K. Here, the angular dependence of $1/T_1T$ at 2.4 K in the 2.1 K sample is thought to arise from the deviation between the directions of \mathbf{H}_{ext} and the effective magnetic field $\mathbf{H}_{\text{eff}} = \mathbf{H}_{\text{ext}} + \mathbf{H}_{\text{hf}}$ due to the anisotropy of the Knight shift, similarly to the case of the angular dependence of the Knight shift. As shown in the solid curve of Fig. 6, the angular dependence of $1/T_1T$ in the ab plane can be well explained by the following equation:

$$\frac{1}{T_1T}(\theta_{ba}) = \left(\frac{1}{T_1T}\right)_{H\parallel b} \cos^2 \theta' + \left(\frac{1}{T_1T}\right)_{H\parallel a} \sin^2 \theta'. \quad (7)$$

Here, $\theta' = \tan^{-1}\left(\frac{1+K_a}{1+K_b} \tan \theta_{ba}\right)$ is the angle between \mathbf{H}_{eff} and the b axis.

D. Summary of low-temperature magnetic properties

Finally, we summarize how the magnetic properties are different between the 1.6 K and 2.1 K samples. The static magnetic susceptibility and high-temperature magnetic fluctuations are relatively unaffected by the enhancement of sample quality. However, the distribution of a -axis magnetic susceptibility and $1/T_1T$ in $H \parallel b$ exhibit significant differences between the samples. This supports the presence of slow magnetic fluctuations induced by the U deficiency, as previously proposed in the literature[40]. Such slow fluctuations might be related to the residual electronic term in the specific measurement. These results indicate that in UTe_2 , the quality of the sample is quite important to reveal the effective interaction for superconductivity. The improvement in sample quality also extends the region of the high-field SC phase[33, 66], suggesting that measurements of magnetic properties on the 2.1 K sample will provide insight into the origin of the high-field SC phase. Moreover, we found that the angular rotation in the ab and ac planes does not exhibit the ordinary angular dependence and that a higher-order $\sin^2 2\theta$ term appears below 40 K, which is related to huge magnetic anisotropy in UTe_2 .

IV. CONCLUSION

In conclusion, we performed ^{125}Te -NMR measurements in the ultra-clean 2.1 K sample of UTe_2 and compared the results with those in the 1.6 K sample to investigate the intrinsic magnetic properties of UTe_2 . The enhancement of the linewidth of the NMR spectrum in the a -axis magnetic field and the low-temperature magnetic fluctuations observed in the 1.6 K sample are suppressed in the 2.1 K sample, suggesting that a tiny amount of U deficiency induces such anomalous magnetic properties. Our findings highlight the importance of high-quality samples for investigating the essential magnetic and SC properties of UTe_2 .

ACKNOWLEDGMENTS

We acknowledge S. Yonezawa and Y. Yanase for fruitful discussion. This work was supported by Grants-in-Aid for Scientific Research (KAKENHI Grant No. JP20KK0061, No. JP20H00130, No. JP21K18600, No. JP22H04933, No. JP22H01168, No. JP23H01124, No. JP23K22439 and No. JP23K25821) from the Japan Society for the Promotion of Science, by JST SPRING(Grant No. JPMJSP2110) from the Japan Science and Technology Agency, by research support funding from the Kyoto University Foundation, by ISHIZUE 2024 of Kyoto University Research Development Program, by Murata Science and Education Foundation, and by the JGC-S Scholarship Foundation. Liquid helium is supplied by

the Low Temperature and Materials Sciences Division, Agency for Health, Safety and Environment, Kyoto Uni-

versity.

H.M. and S.K. equally contributed to this work.

* matsumura.hiroki.75r@st.kyoto-u.ac.jp

† kitagawa.shunsaku.8u@kyoto-u.ac.jp

- [1] J. Bardeen, L. N. Cooper, and J. R. Schrieffer, Theory of superconductivity, *Phys. Rev.* **108**, 1175 (1957).
- [2] T. Moriya and K. Ueda, Spin fluctuations and high temperature superconductivity, *Adv. Phys.* **49**, 555 (2000).
- [3] T. Moriya and K. Ueda, Antiferromagnetic spin fluctuation and superconductivity, *Rep. Prog. Phys.* **66**, 1299 (2003).
- [4] P. Monthoux, A. V. Balatsky, and D. Pines, Toward a theory of high-temperature superconductivity in the antiferromagnetically correlated cuprate oxides, *Phys. Rev. Lett.* **67**, 3448 (1991).
- [5] C. Pfleiderer, Superconducting phases of *f*-electron compounds, *Rev. Mod. Phys.* **81**, 1551 (2009).
- [6] Y. Nakai, T. Iye, S. Kitagawa, K. Ishida, S. Kasahara, T. Shibauchi, Y. Matsuda, H. Ikeda, and T. Terashima, Normal-state spin dynamics in the iron-pnictide superconductors $\text{BaFe}_2(\text{As}_{1-x}\text{P}_x)_2$ and $\text{Ba}(\text{Fe}_{1-x}\text{Co}_x)_2\text{As}_2$ probed with NMR measurements, *Phys. Rev. B* **87**, 174507 (2013).
- [7] S. Kitagawa, T. Kawamura, K. Ishida, Y. Mizukami, S. Kasahara, T. Shibauchi, T. Terashima, and Y. Matsuda, Universal relationship between low-energy antiferromagnetic fluctuations and superconductivity in $\text{BaFe}_2(\text{As}_{1-x}\text{P}_x)_2$, *Phys. Rev. B* **100**, 060503(R) (2019).
- [8] V. P. Mineev, Superconductivity in uranium ferromagnets, *Phys.-Uspek.* **60**, 121 (2017).
- [9] M. Manago, S. Kitagawa, K. Ishida, K. Deguchi, N. K. Sato, and T. Yamamura, Spin-triplet superconductivity in the paramagnetic UCoGe under pressure studied by ^{59}Co NMR, *Phys. Rev. B* **100**, 035203 (2019).
- [10] K. Ishida, S. Matsuzaki, M. Manago, T. Hattori, S. Kitagawa, M. Hirata, T. Sasaki, and D. Aoki, Pairing interaction in superconducting UCoGe tunable by magnetic field, *Phys. Rev. B* **104**, 144505 (2021).
- [11] S. Kitagawa, M. Kibune, K. Kinjo, M. Manago, T. Taniguchi, K. Ishida, M. Brando, E. Hassinger, C. Geibel, and S. Khim, Two-dimensional XY-type Magnetic Properties of Locally Noncentrosymmetric Superconductor CeRh_2As_2 , *J. Phys. Soc. Jpn.* **91**, 043702 (2022).
- [12] S. Ogawa, T. Miyoshi, K. Matano, S. Kawasaki, Y. Inada, and G.-q. Zheng, Single crystal growth of and hyperfine couplings in the spin-triplet superconductor $\text{K}_2\text{Cr}_3\text{As}_3$, *J. Phys. Soc. Jpn.* **92**, 064711 (2023).
- [13] H. Sato, M. Akatsu, R. Kurihara, Y. Kobayashi, and Y. Nemoto, Observation of ferroquadrupole quantum criticality in iron pnictide superconductor $\text{Ba}(\text{Fe}_{1-x}\text{Co}_x)_2\text{As}_2$, *J. Phys. Soc. Jpn.* **92**, 124710 (2023).
- [14] K. Omasa, T. Komoda, Y. Nakamura, E. Matsuoka, H. Kotegawa, H. Tou, T. Sakurai, H. Ohta, A. Nakamura, Y. Homma, D. Aoki, D. Satoh, M. Yoshida, S. Mishra, I. Sheikin, H. Harima, and H. Sugawara, Superconducting and Fermi surface properties of a valence fluctuation compound CeIr_2 , *J. Phys. Soc. Jpn.* **93**, 034704 (2024).
- [15] S. Ran, C. Eckberg, Q.-P. Ding, Y. Furukawa, T. Metz, S. R. Saha, I.-L. Liu, M. Zic, H. Kim, J. Paglione, and N. P. Butch, Nearly ferromagnetic spin-triplet superconductivity, *Science* **365**, 684 (2019).
- [16] D. Aoki, A. Nakamura, F. Honda, D. Li, Y. Homma, Y. Shimizu, Y. J. Sato, G. Knebel, J.-P. Brison, A. Pourret, D. Braithwaite, G. Lapertot, Q. Niu, M. Vališka, H. Harima, and J. Flouquet, Unconventional superconductivity in heavy fermion UTe_2 , *J. Phys. Soc. Jpn.* **88**, 043702 (2019).
- [17] D. Aoki, J.-P. Brison, J. Flouquet, K. Ishida, G. Knebel, Y. Tokunaga, and Y. Yanase, Unconventional superconductivity in UTe_2 , *J. Phys.: Cond. Matt.* **34**, 243002 (2022).
- [18] S. S. Saxena, P. Agarwal, K. Ahilan, F. M. Grosche, R. K. W. Haselwimmer, M. J. Steiner, E. Pugh, I. R. Walker, S. R. Julian, P. Monthoux, G. G. Lonzarich, A. Huxley, I. Sheikin, D. Braithwaite, and J. Flouquet, Superconductivity on the border of itinerant-electron ferromagnetism in UGe_2 , *Nature* **406**, 587 (2000).
- [19] D. Aoki, A. Huxley, E. Ressouche, D. Braithwaite, J. Flouquet, J.-P. Brison, E. Lhotel, and C. Paulsen, Coexistence of superconductivity and ferromagnetism in URhGe , *Nature* **413**, 613 (2001).
- [20] N. T. Huy, A. Gasparini, D. E. de Nijs, Y. Huang, J. C. P. Klaasse, T. Gortenmulder, A. de Visser, A. Hamann, T. Görlach, and H. v. Löhneysen, Superconductivity on the border of weak itinerant ferromagnetism in UCoGe , *Phys. Rev. Lett.* **99**, 067006 (2007).
- [21] D. Aoki, K. Ishida, and J. Flouquet, Review of u-based ferromagnetic superconductors: Comparison between UGe_2 , URhGe , and UCoGe , *J. Phys. Soc. Jpn.* **88**, 022001 (2019).
- [22] G. Knebel, W. Knafo, A. Pourret, Q. Niu, M. Vališka, D. Braithwaite, G. Lapertot, M. Nardone, A. Zitouni, S. Mishra, I. Sheikin, G. Seyfarth, J.-P. Brison, D. Aoki, and J. Flouquet, Field-reentrant superconductivity close to a metamagnetic transition in the heavy-fermion superconductor UTe_2 , *J. Phys. Soc. Jpn.* **88**, 063707 (2019).
- [23] G. Knebel, M. Kimata, M. Vališka, F. Honda, D. Li, D. Braithwaite, G. Lapertot, W. Knafo, A. Pourret, Y. J. Sato, Y. Shimizu, T. Kihara, J.-P. Brison, J. Flouquet, and D. Aoki, Anisotropy of the upper critical field in the heavy-fermion superconductor UTe_2 under pressure, *J. Phys. Soc. Jpn.* **89**, 053707 (2020).
- [24] A. Rosuel, C. Marcenat, G. Knebel, T. Klein, A. Pourret, N. Marquardt, Q. Niu, S. Rousseau, A. Demuer, G. Seyfarth, G. Lapertot, D. Aoki, D. Braithwaite, J. Flouquet, and J. P. Brison, Field-induced tuning of the pairing state in a superconductor, *Phys. Rev. X* **13**, 011022 (2023).
- [25] D. Braithwaite, M. Vališka, G. Knebel, G. Lapertot, J.-P. Brison, A. Pourret, M. E. Zhitomirsky, J. Flouquet, F. Honda, and D. Aoki, Multiple superconducting phases in a nearly ferromagnetic system, *Commun. Phys.* **2**, 147 (2019).
- [26] D. Aoki, F. Honda, G. Knebel, D. Braithwaite, A. Nakamura, D. Li, Y. Homma, Y. Shimizu, Y. J. Sato, J.-P. Bri-

- son, and J. Flouquet, Multiple superconducting phases and unusual enhancement of the upper critical field in UTe_2 , *J. Phys. Soc. Jpn.* **89**, 053705 (2020).
- [27] S. Ran, I.-L. Liu, Y. S. Eo, D. J. Campbell, P. M. Neves, W. T. Fuhrman, S. R. Saha, C. Eckberg, H. Kim, D. Graf, F. Balakirev, J. Singleton, J. Paglione, and N. P. Butch, Extreme magnetic field-boosted superconductivity, *Nat. Phys.* **15**, 1250 (2019).
- [28] W. Knafo, M. Nardone, M. Vališka, A. Zitouni, G. Lapertot, D. Aoki, G. Knebel, and D. Braithwaite, Comparison of two superconducting phases induced by a magnetic field in UTe_2 , *Commun. Phys.* **4**, 40 (2021).
- [29] H. Sakai, Y. Tokiwa, P. Opletal, M. Kimata, S. Awaji, T. Sasaki, D. Aoki, S. Kambe, Y. Tokunaga, and Y. Haga, Field induced multiple superconducting phases in UTe_2 along hard magnetic axis, *Phys. Rev. Lett.* **130**, 196002 (2023).
- [30] K. Kinjo, H. Fujibayashi, S. Kitagawa, K. Ishida, Y. Tokunaga, H. Sakai, S. Kambe, A. Nakamura, Y. Shimizu, Y. Homma, D. X. Li, F. Honda, D. Aoki, K. Hiraki, M. Kimata, and T. Sasaki, Change of superconducting character in UTe_2 induced by magnetic field, *Phys. Rev. B* **107**, L1060502 (2023).
- [31] K. Kinjo, H. Fujibayashi, H. Matsumura, F. Hori, S. Kitagawa, K. Ishida, Y. Tokunaga, H. Sakai, S. Kambe, A. Nakamura, Y. Shimizu, Y. Homma, D. Li, F. Honda, and D. Aoki, Superconducting spin reorientation in spin-triplet multiple superconducting phases of UTe_2 , *Sci. Adv.* **9**, adg2736 (2023).
- [32] M. O. Ajeesh, J. D. Thompson, E. D. Bauer, F. Ronning, S. M. Thomas, and P. F. S. Rosa, Hydrostatic pressure studies on non-superconducting UTe_2 , *J. Phys. Soc. Jpn.* **93**, 055001 (2024).
- [33] D. Aoki, I. Sheikin, N. Marquardt, G. Lapertot, J. Flouquet, and G. Knebel, High field superconducting phases of ultra clean single crystal UTe_2 , *J. Phys. Soc. Jpn.* **93**, 123702 (2024).
- [34] Y. Tokunaga, H. Sakai, S. Kambe, T. Hattori, N. Higa, G. Nakamine, S. Kitagawa, K. Ishida, A. Nakamura, Y. Shimizu, Y. Homma, D. Li, F. Honda, and D. Aoki, ^{125}Te -NMR study on a single crystal of heavy fermion superconductor UTe_2 , *J. Phys. Soc. Jpn.* **88**, 073701 (2019).
- [35] S. Sundar, S. Gheidi, K. Akintola, A. M. Côté, S. R. Dunsiger, S. Ran, N. P. Butch, S. R. Saha, J. Paglione, and J. E. Sonier, Coexistence of ferromagnetic fluctuations and superconductivity in the actinide superconductor UTe_2 , *Phys. Rev. B* **100**, 140502(R) (2019).
- [36] Y. Tokunaga, H. Sakai, S. Kambe, P. Opletal, Y. Tokiwa, Y. Haga, S. Kitagawa, K. Ishida, D. Aoki, G. Knebel, G. Lapertot, S. Krämer, and M. Horvatić, Longitudinal spin fluctuations driving field-reinforced superconductivity in UTe_2 , *Phys. Rev. Lett.* **131**, 226503 (2023).
- [37] C. Duan, K. Sasmal, M. B. Maple, A. Podlesnyak, J.-X. Zhu, Q. Si, and P. Dai, Incommensurate spin fluctuations in the spin-triplet superconductor candidate UTe_2 , *Phys. Rev. Lett.* **125**, 237003 (2020).
- [38] W. Knafo, G. Knebel, P. Steffens, K. Kaneko, A. Rosuel, J.-P. Brison, J. Flouquet, D. Aoki, G. Lapertot, and S. Raymond, Low-dimensional antiferromagnetic fluctuations in the heavy-fermion paramagnetic ladder compound UTe_2 , *Phys. Rev. B* **104**, L100409 (2021).
- [39] W. Knafo, T. Thebault, P. Manuel, D. D. Khalyavin, F. Orlandi, E. Ressouche, K. Beauvois, G. Lapertot, K. Kaneko, D. Aoki, D. Braithwaite, G. Knebel, and S. Raymond, Incommensurate antiferromagnetism in UTe_2 under pressure, arXiv:2311.05455. (2023).
- [40] Y. Tokunaga, H. Sakai, S. Kambe, Y. Haga, Y. Tokiwa, P. Opletal, H. Fujibayashi, K. Kinjo, S. Kitagawa, K. Ishida, A. Nakamura, Y. Shimizu, Y. Homma, D. Li, F. Honda, and D. Aoki, Slow electronic dynamics in the paramagnetic state of UTe_2 , *J. Phys. Soc. Jpn.* **91**, 023707 (2022).
- [41] H. Fujibayashi, K. Kinjo, G. Nakamine, S. Kitagawa, K. Ishida, Y. Tokunaga, H. Sakai, S. Kambe, A. Nakamura, Y. Shimizu, Y. Homma, D. Li, F. Honda, and D. Aoki, Low-temperature magnetic fluctuations investigated by ^{125}Te -NMR on the uranium-based superconductor UTe_2 , *J. Phys. Soc. Jpn.* **92**, 053702 (2023).
- [42] S. Sundar, N. Azari, M. R. Goeks, S. Gheidi, M. Abedi, M. Yakovlev, S. R. Dunsiger, J. M. Wilkinson, S. J. Blundell, T. E. Metz, I. M. Hayes, S. R. Saha, S. Lee, A. J. Woods, R. Movshovich, S. M. Thomas, N. P. Butch, P. F. S. Rosa, J. Paglione, and J. E. Sonier, Ubiquitous spin freezing in the superconducting state of UTe_2 , *Commun. Phys.* **6**, 24 (2023).
- [43] K. Momma and F. Izumi, VESTA 3 for three-dimensional visualization of crystal, volumetric and morphology data, *J. Appl. Crystallogr.* **44**, 1272 (2011).
- [44] H. Matsumura, H. Fujibayashi, K. Kinjo, S. Kitagawa, K. Ishida, Y. Tokunaga, H. Sakai, S. Kambe, A. Nakamura, Y. Shimizu, Y. Homma, D. Li, F. Honda, and D. Aoki, Large reduction in the a -axis Knight shift on UTe_2 with $T_c = 2.1$ K, *J. Phys. Soc. Jpn.* **92**, 063701 (2023).
- [45] H. Sakai, P. Opletal, Y. Tokiwa, E. Yamamoto, Y. Tokunaga, S. Kambe, and Y. Haga, Single crystal growth of superconducting UTe_2 by molten salt flux method, *Phys. Rev. Mater.* **6**, 073401 (2022).
- [46] D. Li, A. Nakamura, F. Honda, Y. J. Sato, Y. Homma, Y. Shimizu, J. Ishizuka, Y. Yanase, G. Knebel, J. Flouquet, and D. Aoki, Magnetic properties under pressure in novel spin-triplet superconductor UTe_2 , *J. Phys. Soc. Jpn.* **90**, 073703 (2021).
- [47] D. Aoki, Molten salt flux liquid transport method for ultra clean single crystals UTe_2 , *J. Phys. Soc. Jpn.* **93**, 043703 (2024).
- [48] P. Opletal, H. Sakai, Y. Haga, Y. Tokiwa, E. Yamamoto, S. Kambe, and Y. Tokunaga, Ferromagnetic crossover within the ferromagnetic order of U_7Te_{12} , *J. Phys. Soc. Jpn.* **92**, 034704 (2023).
- [49] D. Aoki, H. Sakai, P. Opletal, Y. Tokiwa, J. Ishizuka, Y. Yanase, H. Harima, A. Nakamura, D. Li, Y. Homma, Y. Shimizu, G. Knebel, J. Flouquet, and Y. Haga, First observation of the de Haas-van Alphen effect and fermi surfaces in the unconventional superconductor UTe_2 , *J. Phys. Soc. Jpn.* **91**, 083704 (2022).
- [50] Y. Haga, P. Opletal, Y. Tokiwa, E. Yamamoto, Y. Tokunaga, S. Kambe, and H. Sakai, Effect of uranium deficiency on normal and superconducting properties in unconventional superconductor UTe_2 , *J. Phys.: Cond. Matt.* **34**, 175601 (2022).
- [51] H. Fujibayashi, G. Nakamine, K. Kinjo, S. Kitagawa, K. Ishida, Y. Tokunaga, H. Sakai, S. Kambe, A. Nakamura, Y. Shimizu, Y. Homma, D. Li, F. Honda, and D. Aoki, Superconducting order parameter in UTe_2 determined by Knight shift measurement, *J. Phys. Soc. Jpn.* **91**, 043705 (2022).

- [52] S. Kitagawa, K. Nakanishi, H. Matsumura, Y. Takahashi, K. Ishida, Y. Tokunaga, H. Sakai, S. Kambe, A. Nakamura, Y. Shimizu, Y. Homma, D. Li, F. Honda, A. Miyake, and D. Aoki, Clear reduction in spin susceptibility and superconducting spin rotation for $H \parallel a$ in the early-stage sample of spin-triplet superconductor UTe_2 , *J. Phys. Soc. Jpn.* **93**, 123701 (2024).
- [53] G. C. Carter, L. H. Bennett, and D. J. Kahan, *Metallic shifts in NMR* (Pergamon Press, Oxford, 1977).
- [54] G. Nakamine, K. Kinjo, S. Kitagawa, K. Ishida, Y. Tokunaga, H. Sakai, S. Kambe, A. Nakamura, Y. Shimizu, Y. Homma, D. Li, F. Honda, and D. Aoki, Anisotropic response of spin susceptibility in the superconducting state of UTe_2 probed with ^{125}Te -NMR measurement, *Phys. Rev. B* **103**, L100503 (2021).
- [55] R. Okazaki, T. Shibauchi, H. J. Shi, Y. Haga, T. D. Matsuda, E. Yamamoto, Y. Onuki, H. Ikeda, and Y. Matsuda, Rotational symmetry breaking in the hidden-order phase of URu_2Si_2 , *Science* **331**, 439 (2011).
- [56] H. Ikeda, M.-T. Suzuki, R. Arita, T. Takimoto, T. Shibauchi, and Y. Matsuda, Emergent rank-5 nematic order in URu_2Si_2 , *Nature Physics* **8**, 528 (2012).
- [57] A. Inda and S. Hayami, Nonlinear transverse magnetic susceptibility under electric toroidal dipole ordering, *J. Phys. Soc. Jpn.* **92**, 043701 (2023).
- [58] S. Hayami and H. Kusunose, Unified description of electronic orderings and cross correlations by complete multipole representation, *J. Phys. Soc. Jpn.* **93**, 072001 (2024).
- [59] D. V. Ambika, Q.-P. Ding, K. Rana, C. E. Frank, E. L. Green, S. Ran, N. P. Butch, and Y. Furukawa, Possible coexistence of antiferromagnetic and ferromagnetic spin fluctuations in the spin-triplet superconductor UTe_2 revealed by ^{125}Te NMR under pressure, *Phys. Rev. B* **105**, L220403 (2022).
- [60] K. Kinjo, H. Fujibayashi, G. Nakamine, S. Kitagawa, K. Ishida, Y. Tokunaga, H. Sakai, S. Kambe, A. Nakamura, Y. Shimizu, Y. Homma, D. Li, F. Honda, and D. Aoki, Drastic change in magnetic anisotropy of UTe_2 under pressure revealed by ^{125}Te -NMR, *Phys. Rev. B* **105**, L140502 (2022).
- [61] K. Willa, F. Hardy, D. Aoki, D. Li, P. Wiecki, G. Lapertot, and C. Meingast, Thermodynamic signatures of short-range magnetic correlations in UTe_2 , *Phys. Rev. B* **104**, 205107 (2021).
- [62] G. Knebel, A. Pourret, S. Rousseau, N. Marquardt, D. Braithwaite, F. Honda, D. Aoki, G. Lapertot, W. Knafo, G. Seyfarth, J.-P. Brison, and J. Flouquet, c -axis electrical transport at the metamagnetic transition in the heavy-fermion superconductor UTe_2 under pressure, *Phys. Rev. B* **109**, 155103 (2024).
- [63] Y. Tokiwa, P. Opletal, H. Sakai, S. Kambe, E. Yamamoto, M. Kimata, S. Awaji, T. Sasaki, D. Aoki, Y. Haga, and Y. Tokunaga, Reinforcement of superconductivity by quantum critical fluctuations of metamagnetism in UTe_2 , *Phys. Rev. B* **109**, L140502 (2024).
- [64] N. Azari, M. Yakovlev, N. Rye, S. R. Dunsiger, S. Sundar, M. M. Bordelon, S. M. Thomas, J. D. Thompson, P. F. S. Rosa, and J. E. Sonier, Absence of spontaneous magnetic fields due to time-reversal symmetry breaking in bulk superconducting UTe_2 , *Phys. Rev. Lett.* **131**, 226504 (2023).
- [65] T. Hattori, Y. Ihara, Y. Nakai, K. Ishida, Y. Tada, S. Fujimoto, N. Kawakami, E. Osaki, K. Deguchi, N. K. Sato, and I. Satoh, Superconductivity induced by longitudinal ferromagnetic fluctuations in $UCoGe$, *Phys. Rev. Lett.* **108**, 066403 (2012).
- [66] Z. Wu, T. I. Weinberger, J. Chen, A. Cabala, D. V. Chichinadze, D. Shaffer, J. Pospíšil, J. Prokleška, T. Haidamak, G. Bastien, V. Sechovsky, A. J. Hickey, M. J. Mancera-Ugarte, S. Benjamin, D. E. Graf, Y. Skourski, G. G. Lonzarich, M. Vališka, F. M. Grosche, and A. G. Eaton, Enhanced triplet superconductivity in next-generation ultraclean UTe_2 , *Proc. Natl. Acad. Sci.* **121**, e2403067121 (2024).